Infrared Physics & Technology 55 (2012) 19–25

Contents lists available at SciVerse ScienceDirect

Infrared Physics & Technology

journal homepage: www.elsevier.com/locate/infrared

Tensor diffusion level set method for infrared targets contours extraction ☆

Meng Li [a,*], Chuanjiang He [a], Yi Zhan [b]

[a] College of Mathematics and Statistics, Chongqing University, Chongqing 400044, PR China
[b] College of Mathematics and Statistics, Chongqing Technology and Business University, Chongqing 400067, PR China

ARTICLE INFO

Article history:
Received 19 December 2010
Available online 13 September 2011

Keywords:
Contours extraction
Variational level set method
Structure tensor
Tensor diffusion
Infrared image

ABSTRACT

A tensor diffusion level set method is presented to extract infrared (IR) targets contour under a sky–mountain–water complex background. The proposed model combines tensor diffusion operator and the eigenvalues of tensor-image into a common energy minimization level set framework. By incorporating the information of image tensor diffusion operator into the external energy term, the level set function can move in a specific way. And eigenvalues of tensor-image are used for the regularization of zero level curves in order to diminish the influence of image 'clutter' and noise. An additional benefit of the proposed method is robust to initial conditions. Experimental results show very good performance of the tensor diffusion level set method for IR targets contours extraction.

1. Introduction

As a key technique in infrared (IR) alert and automatic target recognition system, IR targets detection has became one of the most important topics in the field of IR image processing [1]. However, IR targets detection is yet a difficult task. This difficult can be arises from the fact that most IR images are characterized by complex background. Various techniques have been proposed for IR target detection. These methods include: thresholding algorithm [2,3], wavelet transformation [4,5], stochastic algorithm [6] and real-time detection method [7], etc. Recently, variational level set method [8–10], which express targets detection as the minimization of a functional, have been well established and widely used in various image applications, including IR targets contours extraction [11,12] and medical image segmentation [13,14]. The main advantages of this method is that the variational models can be easily formulated under a principled energy minimization framework, and allow incorporation of various prior knowledge, such as shape and intensity distribution, for robust image segmentation [10]. This paper will focus on variational level set methods for IR targets contours extraction.

In image processing and computer vision applications, the level set method [15] was first introduced independently by Caselles et al. [16] and Malladi et al. [17] in the context of active contours for image segmentation. The original idea is to implicitly represent an interface as the zero level set of a function in higher dimension, referred as to a level set function, and then the level set function is deformed according to an evolution partial differential equation (PDE). A remarkable merit is that the level set function evolution allows for cusps, corners, and automatic topological change of active contour. Variational level set methods for image segmentation involve minimizing an energy functional over a space of level set functions using continuous gradient descent method. The energy functional typically includes the internal energy that smoothes the level set function and the external energy that drives the motion of the zero level set toward the desired image features, such as objects boundaries.

However, the previous level set-based works on IR targets contours extraction [11,12] represent an image by a scalar or vector in dimensional space. In so doing, some useful information in the original data may not be captured well. As a consequence, these approaches typically experience difficulty handling images with a significant portion of mixed pixels. In fact, pixel mixing often occurs in real IR images from different modalities. By reason of light or sun, some regions in background can produce higher gray-level than objects, this phenomenon is called 'pixel mixing' or 'clutter'. Generally, 'clutter' can be seen as a special noise.

Recently, a number of algorithms for image processing with structure tensor and tensor anisotropic diffusion have been proposed and attracted great interest [18–21]. Structure tensor and tensor diffusion directly treats the data as tensor, and thus effectively avoids the problems derived from treating data as scalars or vectors. This construction indeed allows for smoothing along discontinuities of the tensor field, while smoothing across discontinuities is inhibited [18]. In most applications, especially for IR image segmentation, it is desirable that there is a filling-in effect of local information.

In this paper, we propose a tensor diffusion level set method to extract IR targets contour. The proposed model combines tensor

☆ This work is supported by the Fundamental Research Funds of the Central Universities (CDJXS11101134) and Natural Science Foundation Project of CQ CSTC (cstcjjA40012).

* Corresponding author.
E-mail address: limeng7319@yahoo.cn (M. Li).

1350-4495/$ - see front matter © 2011 Elsevier B.V. All rights reserved.
doi:10.1016/j.infrared.2011.08.009

diffusion operator and the eigenvalues of tensor-image into a common energy minimization level set framework. By incorporating the information of image tensor diffusion operator into the external energy term, the level set function moves up or down in transition region. And the zero level curves can be generated automatically at image locations which encounter two opposite directions of flow. In addition, a weighted $p(\lambda_1,\lambda_2)$-Dirichlet integral as regularity term is presented to diminish the influence of image 'clutter' and noise. So the targets contours in IR image with complex background can be efficiently extraction. The tensor diffusion level set method has an added benefit of allowing the use of a more simple level set initialization scheme, i.e., the level set function can be initialized with a constant function. It is more easier to use in practice than the widely used signed distance function or binary function.

The remainder of this paper is organized as follows. In Section 2, we review the structure tensor and tensor diffusion. The proposed model is introduced in Section 3. Numerical algorithms and experimental results are presented in Section 4. This paper is summarized in Section 5.

2. The structure tensor and tensor diffusion

For a scalar image I, the classical structure tensor D is defined by Gaussian smoothing of the tensor product of the image gradient, i.e. [18]:

$$D = J_\sigma(\nabla I) = G_\sigma * (\nabla I \nabla I^T) = \begin{pmatrix} G_\sigma * I_x^2 & G_\sigma * I_x I_y \\ G_\sigma * I_x I_y & G_\sigma * I_y^2 \end{pmatrix} \tag{1}$$

where ∇ is gradient operator, G_σ is a Gaussian kernel with standard deviation σ, and subscripts x and y denote the partial derivatives. Since the structure tensor is symmetric and semi-positive definite matrix for each point $(x,y) \in \Omega$, the eigenvalues (λ_1, λ_2, where $\lambda_1 \geqslant \lambda_2$) are always non-negative. Its orthogonal eigenvectors υ_1 and eigenvectors υ_2 provide the preferred local structure, and the corresponding eigenvalues λ_1 and λ_2 provide the average contrast along υ_1 and υ_2, respectively. This means that υ_1 is the orientation with the highest gray value fluctuations and υ_2 the preferred local orientation. Constant areas in image are characterized by $\lambda_1 = \lambda_2 = 0$, local structure with larger variation, for example edge transition region, give $\lambda_1 \gg \lambda_2 \approx 0$, corners can be identified by $\lambda_1 \geqslant \lambda_2 \gg 0$.

Meanwhile, Weickert proposed a tensor diffusion in image processing [18],

$$\frac{\partial I}{\partial t} = div(D\nabla I) \tag{2}$$

where $div(\cdot)$ is divergence operator, and $D \in R^{2\times 2}$ is a symmetric positive semi-definite diffusion tensor. With the tensor structure D, we call the divergence operator $div(D\nabla I)$ as a tensor diffusion operator.

By diagonalizing the structure tensor D, the structure tensor can be described in terms of its eigenvalues and orthogonal unit eigenvectors:

$$D = (\upsilon_1, \upsilon_2) \begin{pmatrix} \lambda_1 & 0 \\ 0 & \lambda_2 \end{pmatrix} \begin{pmatrix} \upsilon_1^T \\ \upsilon_2^T \end{pmatrix} \tag{3}$$

Under local coordinate system (υ_1, υ_2),

$$\nabla I = \frac{\partial I}{\partial \upsilon_1}\upsilon_1 + \frac{\partial I}{\partial \upsilon_2}\upsilon_2 \tag{4}$$

and the Eq. (2) can be rewritten as

$$\frac{\partial I}{\partial t} = \frac{\partial}{\partial \upsilon_1}\left(\lambda_1 \frac{\partial I}{\partial \upsilon_1}\right) + \frac{\partial}{\partial \upsilon_2}\left(\lambda_2 \frac{\partial I}{\partial \upsilon_2}\right) \tag{5}$$

So the Eq. (2) provides the anisotropic diffusion in the true sense. In this anisotropic case not only the diffusion is adapted locally to the data but also the direction of smoothing.

3. Tensor diffusion level set model

In this section, we propose a tensor diffusion level set evolution strategy in terms of tensor diffusion operator and the eigenvalues of tensor-image. The goal is to automatic extract the IR targets contours under a sky–mountain–water complex background. The overall energy functional in our proposed model consists of three parts: external energy term $E_{ext}(\phi)$, regularity term $E_{reg}(\phi)$ and internal energy term $P(\phi)$, Thus the overall energy functional can be described as

$$E(\phi) = \nu E_{ext}(\phi) + \lambda E_{reg}(\phi) + \mu P(\phi) \tag{6}$$

where ν, λ, $\mu > 0$ are constants. When the zero level set of ϕ finally comes to a steady state, it will become the contours that separate IR objects from the background.

For a given image I: $\Omega \to R$ and a level set function $\phi(x,y)$: $\Omega \to R$, where $\Omega \subset R^2$ is the image domain, we first formulate the external energy $E_{ext}(\phi)$ as:

$$E_{ext}(\phi) = \int_\Omega div(J_\sigma(\nabla I)\nabla I) \cdot H_\varepsilon(-\phi)dx\,dy \tag{7}$$

and

$$H_\varepsilon(z) = \frac{1}{2}\left(1 + \frac{2}{\pi}\arctan\left(\frac{z}{\varepsilon}\right)\right) \tag{8}$$

$$J_\sigma(\nabla I) = G_\sigma * (\nabla I \nabla I^T) = \begin{pmatrix} G_\sigma * I_x^2 & G_\sigma * I_x I_y \\ G_\sigma * I_x I_y & G_\sigma * I_y^2 \end{pmatrix} \tag{9}$$

where $H_\varepsilon(\cdot)$ is the smooth Heaviside function defined by [8].

In order to control the smoothness of the zero level set and further avoid the occurrence of small, isolated regions in the final segmentation, we construct the following functional as the geometric regularization on the zero level set:

$$E_{reg}(\phi) = \int_\Omega \frac{1}{p(\lambda_1,\lambda_2)}\delta_\varepsilon(\phi)|\nabla\phi|^{p(\lambda_1,\lambda_2)}dx\,dy \tag{10}$$

and

$$\delta_\varepsilon(z) = H'_\varepsilon(z) = \frac{1}{\pi}\frac{\varepsilon}{\varepsilon^2 + z^2} \tag{11}$$

$$p(\lambda_1,\lambda_2) = \begin{cases} 1 & if\ \lambda_1 \geqslant \lambda_2 > K \\ 1 + \frac{1}{2}\exp(-(\lambda_1 - \lambda_2)^2) & otherwise \end{cases} \tag{12}$$

where $\delta_\varepsilon(\cdot)$ is the smooth Dirac function, λ_1, $\lambda_2(\lambda_1 \geqslant \lambda_2)$ are eigenvalues of the structure tensor $J_\sigma(\nabla I)$, K is a threshold. In this paper, we choose threshold $K = 10$. For each pair λ_1 and λ_2, we have $p(\lambda_1,\lambda_2) \in [1, 1.5]$.

The functional (10) is in fact the weighted p-Dirichlet integral with variable exponent, so we call it the weighted $p(\lambda_1,\lambda_2)$-Dirichlet integral.

In [9], Li et al., proposed an internal energy:

$$P(\phi) = \frac{1}{2}\int_\Omega (|\nabla\phi| - 1)^2\,dx\,dy \tag{13}$$

which acts as a metric to characterize how close the level set function to a signed distance function. This metric will be adopted in our model to make the evolving level set function behave approximately like a signed distance function.

With the above three metrics, the proposed functional (6) can be rewrite as:

$$\begin{aligned} E(\phi) = {} & \nu\int_\Omega div(J_\sigma(\nabla I)\nabla I)\cdot H_\varepsilon(-\phi)dxdy \\ & + \lambda\int_\Omega \frac{1}{p(\lambda_1,\lambda_2)}\delta_\varepsilon(\phi)|\nabla\phi|^{p(\lambda_1,\lambda_2)}dxdy + \frac{1}{2}\mu\int_\Omega (|\nabla\phi| - 1)^2 dxdy \end{aligned} \tag{14}$$

In a dynamical scheme via steepest descent, minimizing the energy functional (14) with respect to ϕ, we obtain the evolution PDE:

$$\frac{\partial\phi}{\partial t}=\delta_\varepsilon(\phi)\left(v div(J_\sigma(\nabla I)\nabla I)+\lambda div(|\nabla\phi|^{p(\lambda_1,\lambda_2)-2}\nabla\phi)\right) -\lambda\left(\frac{1}{p(\lambda_1,\lambda_2)}-1\right)\delta'_\varepsilon(\phi)|\nabla\phi|^{p(\lambda_1,\lambda_2)}+\mu\left(\Delta\phi-div\left(\frac{\nabla\phi}{|\nabla\phi|}\right)\right) \quad (15)$$

3.1. Why use the tensor diffusion operator in external energy term?

In this subsection, we analyze the behavior of external energy functional $E_{ext}(\phi)$ (7). The behavior of $E_{ext}(\phi)$ is mainly controlled by tensor diffusion operator $div(J_\sigma(\nabla I)\nabla I)$. In fact, we have known from Section 2,

$$div(J_\sigma(\nabla I)\nabla I)=\frac{\partial}{\partial\upsilon_1}\left(\lambda_1\frac{\partial I}{\partial\upsilon_1}\right)+\frac{\partial}{\partial\upsilon_2}\left(\lambda_2\frac{\partial I}{\partial\upsilon_2}\right) \quad (16)$$

In image analysis application, the direction υ_1 is considered to be the direction across the image feature, and the direction υ_2 is considered to be the direction along the image feature. According to the properties of λ_1 and λ_2, we have $div(J_\sigma(\nabla I)\nabla I)=0$ for image flat areas. And $div(J_\sigma(\nabla I)\nabla I)\approx\frac{\partial}{\partial\upsilon_1}(\lambda_1\frac{\partial I}{\partial\upsilon_1})$ for image transition region, which indicates that a shift of intensity at image transition region along the direction υ_1 can cause significant response of the operator $div(J_\sigma(\nabla I)\nabla I)$. It is very important for level set evolution.

Let us now investigate the impact of tensor diffusion operator to level set evolution by a simple example for a mollified step edge image (Fig. 1a). In which the level set ϕ evolves according to PDE associated with $E_{ext}(\phi)$ as follows:

$$\frac{\partial\phi}{\partial t}=div(J_\sigma(\nabla I)\nabla I)\delta_\varepsilon(\phi) \quad (17)$$

Fig. 1b shows the 1-D horizontal gray level profiles along the center of the image I, $div(J_\sigma(\nabla I)\nabla I)$, ϕ_0 and ϕ_1. (ϕ_k is ϕ at iteration k). We can seen from Fig. 1b that the operator $div(J_\sigma(\nabla I)\nabla I)$ is positive (negative) in transition region associated with the dark (bright) side of the edge. The level set evolution starts with $\phi_0=1$, and ϕ moves up (down) in transition region associated with the dark (bright) side after 1 iteration. This can easily be explained. $div(J_\sigma(\nabla I)\nabla I)>0$ ($div(J_\sigma(\nabla I)\nabla I)<0$) results in $\frac{\partial\phi}{\partial t}>0(\frac{\partial\phi}{\partial t}<0)$. Then the function ϕ increases (decreases) in transition region, which drives the level set function moving up (down) and causes the sign of ϕ flip around edges. So the zero level curves can be generated automatically at image locations where two opposite directions of flow encounter after iteration k.

3.2. Why use the weighted $p(\lambda_1,\lambda_2)$-Dirichlet integral regularization?

Level set methods must impose some regularization constraints on level set functions usually due to noise. Typically this is performed by penalizing the length or weighted length of the zero level set [8–10]. But its level lines tend to overlap for noisy image [22]. In [22], two smoother regularizations $\int_\Omega|\nabla\phi|^2\,dxdy$ and $\||\nabla\phi|\|_{L^\infty(\Omega)}$ were introduced. They have exhibited certain capability of dealing with noise image and allow the level lines to remain smoothing. However the smoother regularization may cause the active contours to pass through weak object boundary. Recently, Zhou et al. [23] proposed a weighted p-Dirichlet integral as the geometric regularization on zero level set. Different value of $p\geqslant 1$ results in a tradeoff between length regularization and smoother regularization. But if the image intensities representing background are 'clutter', this regularization may become sensitive to exponent p.

Here we introduce the $p(\lambda_1,\lambda_2)$-Dirichlet integral regularization, just as formula (10). The idea behind (10) is that the amount of regularization on zero level set can be adjusted automatically by the exponent $p(\lambda_1,\lambda_2)$ to fit the image feature. Under this situation of the regularization on zero level set, three distinct cases are considered. (1) If $\lambda_1\approx\lambda_2\approx 0$, the local area is considered as foreground or background area. In this case, $p(\lambda_1,\lambda_2)\to 1.5$, which ensures $p(\lambda_1,\lambda_2)$-Dirichlet integral similar to the smoother regularization. This regularization avoids occurrence of small, isolated regions in the final segmentation. (2) If $\lambda_1\gg\lambda_2\approx 0$, the local neighborhood is edge-shaped. Obvious, $p(\lambda_1,\lambda_2)\to 1$, this ensures the active contours not to pass through weak object boundary. (3) $\lambda_1\geqslant\lambda_2\gg 0$, this means a corner is presented at this pixel. we put $p(\lambda_1,\lambda_2)=1$, which ensures that the contour of corner will not be destroyed.

3.3. Flexible initialization of level set function

In standard level set methods [8,16,17], it is necessary to initialize the level set function ϕ as a signed distance function (SDF). But

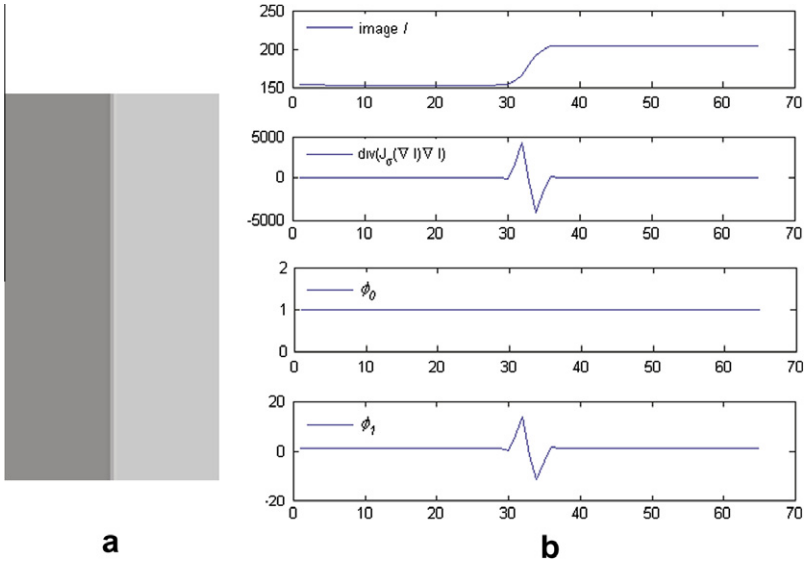

Fig. 1. The contribution of $div(J_\sigma(\nabla I)\nabla I)$ to level set function evolution driven by Eq. (17). (a) Original image I. (b) 1-D horizontal gray level profile along the center of the image I, $div(J_\sigma(\nabla I)\nabla I)$, ϕ_0 and ϕ_1.

such initialization is fraught with its own problems, such as how and where to define the initial contours. Some techniques for automatic or optimal initialization have been proposed [24,25] to address this problem. Recently, an efficient binary initialization scheme was proposed [9] and attracted great interest. However, it still need user intervention to define the initial contours, which limits its applications in practice. Li et al. [26] proposed a nonzero constant initialization scheme to address the problem of contours initialization. In this paper, due to the introduction of the external energy functional (7), the level set function ϕ allows adopting more flexible initialization scheme as follows:

1. The initial level set function is a nonzero constant function [26], such as

$$\phi_0(x,y) = \rho, (x,y) \in \Omega \tag{18}$$

where ρ is a nonzero constant.

2. The initial level set function is a signed distance function [8], such as

$$\phi_0(x,y,t) = \begin{cases} -d((x,y),C), & (x,y) \in in(C) \\ 0, & (x,y) \in C \\ +d((x,y),C), & (x,y) \in out(C) \end{cases} \tag{19}$$

where $d((x,y),C)$ denotes the (shortest) Euclidean distance from the point (x,y) to the curve $C(t)$.

3. The initial level set function is a binary function [9], such as

$$\phi_0(x,y) = \begin{cases} -\rho, & (x,y) \in \omega \\ +\rho, & (x,y) \in \Omega \setminus \omega \end{cases} \tag{20}$$

where ω is a region in the image domain Ω, and $\rho > 0$ is a constant.

To demonstrate effectiveness of the proposed initial scheme, we apply the proposed initialization and tensor-value diffusion level set model for the same image in Fig. 2. The level set evolution starts with the following three case: (1) a nonzero constant level set function; (2) a signed distance function; (3) a binary function. As can be seen, the 3-D plot of initial level set function, the initial contours, the segmentation results and the 3-D plot of final level set function are shown in the first, second, third and forth column of Fig. 2, respectively. Especially for the first case, the level set function is initialized as a nonzero constant level set function, so there is no initial contour. Though we adopt different initial schemes and initial contours, it can be clearly seen from the results in Fig. 2 that we obtain the same desirable results. This experiment also shows that our method robust to initial conditions.

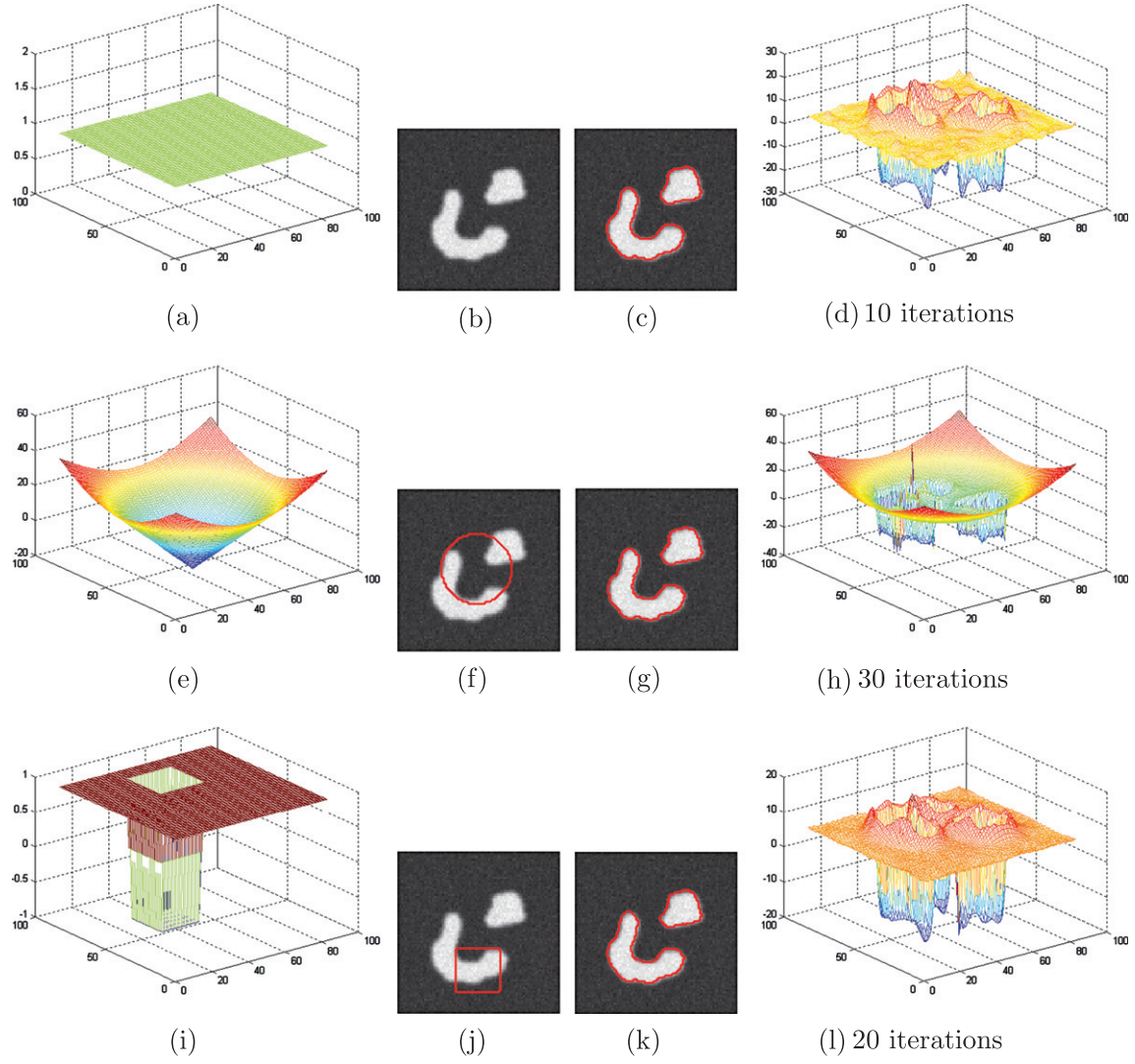

Fig. 2. Tensor diffusion level set evolution with different initial conditions. The first column: 3-D figure of initial level set functions (18)–(20) (from top to bottom), respectively. The second column: Initial contours correspond to different initial scheme. The third column: Final results of contours extraction. The forth column: 3-D figure of final level set functions.

It is worth noting that the constant initial scheme (18) can faster capture the targets contours (only 10 iterations) than the other two initial scheme (30 or 20 iterations), and this kind of constant initial scheme are more easier to use in practice than the widely used signed distance function or binary function. So the level set functions always are simply initialized to a nonzero constant function, i.e. $\phi_0(x,y) = 1$, for later experiments.

4. Numerical algorithm and experimental results

4.1. Implementation

The evolution Eq. (15) is implemented using a simple finite difference scheme. And all the spatial partial derivatives $\partial\phi/\partial x$ and $\partial\phi/\partial y$ are approximated by the central difference, and the temporal partial derivative $\partial\phi/\partial t$ is discretized as the forward difference. The approximation of Eq. (15) can be simply written as

$$\phi_{i,j}^{n+1} = \phi_{i,j}^{n} + \Delta t \cdot L\left(\phi_{i,j}^{n}\right) \tag{21}$$

where $\phi_{i,j}^{n} = \phi(i,j,n\Delta t)$ with $n \geqslant 0$, and $L\left(\phi_{i,j}^{n}\right)$ is the spatial difference approximation of the right hand side in Eq. (15).

Computational cost is also important for level set evolution. In our method, the regularity of the level set function ϕ is inherently ensured by $div(|\nabla\phi|^{p(\lambda_1,\lambda_2)-2}\nabla\phi)$ and $\left(\frac{1}{p(\lambda_1,\lambda_2)}-1\right)\delta_\varepsilon'(\phi)|\nabla\phi|^{p(\lambda_1,\lambda_2)}$. To compute more efficiently, the later can be canceled. Therefore in our implementation, we adopt the following modified form of Eq. (15)

$$\frac{\partial\phi}{\partial t} = \delta_\varepsilon(\phi)\left(v div(J_\sigma(\nabla I)\nabla I) + \lambda div(|\nabla\phi|^{p(\lambda_1,\lambda_2)-2}\nabla\phi)\right) + \mu\left(\Delta\phi - div\left(\frac{\nabla\phi}{|\nabla\phi|}\right)\right) \tag{22}$$

4.2. Experimental results

The proposed tensor diffusion level set method has been applied to extraction targets in varied infrared image scenes. The level set function $\phi(x,y,t)$ is simply initialized to $\phi_0(x,y) = 1$ for all experiments. Besides, we use the following default setting of the parameters for all the experiments: $\varepsilon = 1.5$, $\sigma = 1.5$, $\mu = 0.04$, $\lambda = 10$ and time step $\Delta t = 5.0$. We use relatively small parameter v for the experiment in this section. In general, our method with a smaller value v can produce less sensitivity to 'clutter', while it is more robustness to weak object boundary when a larger v is used. The full decision of value v depends on varied infrared image scenes. We will give the exact value of v each time.

Fig. 3 demonstrates the proposed method effect of several IR images under different 'clutter' background (150×56). All of them are typical image with pixel mixing (see the first column of Fig. 3). Because of the sun's refraction, the waves of the sea produce many high gray-level regions in infrared images. It has been regarded as a difficult task in most case to extract target contours under 'clutter' backgrounds. The second to the forth column in Fig. 3 show how our model works on these images. Level set evolution starts with $\phi_0 = 1$, i.e., there are no initial contours. It can be seen from the second column that some contours can emerge automatically after only 1 iteration. The emergences of contours can be explained as that the external energy term have influence on the change of ϕ in the entire image domain. Afterwards, the generated contours evolve toward the desired objects boundaries, while some false contours in background shrink gradually, as shown in the third and forth column of Fig. 3. This shrinking phenomenon can be interpreted as the influence of the adaptive regularity term. Finally, the evolving curves convergence to the true boundary of each shape after 50 iterations, as can be seen in the forth column of Fig. 3. The results show that our model successfully detects all the IR objects under different 'clutter' backgrounds.

Fig. 4 shows the segmentation results for five real IR images with sky–mountain–water background (250×180) using the 2-D maximum entropy thresholding model [3], the improved CV model [11] and the propose model. In actual sky–mountain–water conflicts, the background of boats were quite complex. Moreover, part of the boats are quite weak. For such image, the 2-D maximum entropy model cannot segment them correctly. In fact, no matter what threshold is selected, some part of the background/foreground is incorrectly identified as the foreground/background, as shown in the second column. The third column of Fig. 4 shows erroneous results obtained by applying the improved CV model. As can be seen, the mountain–water line has a serious impact on

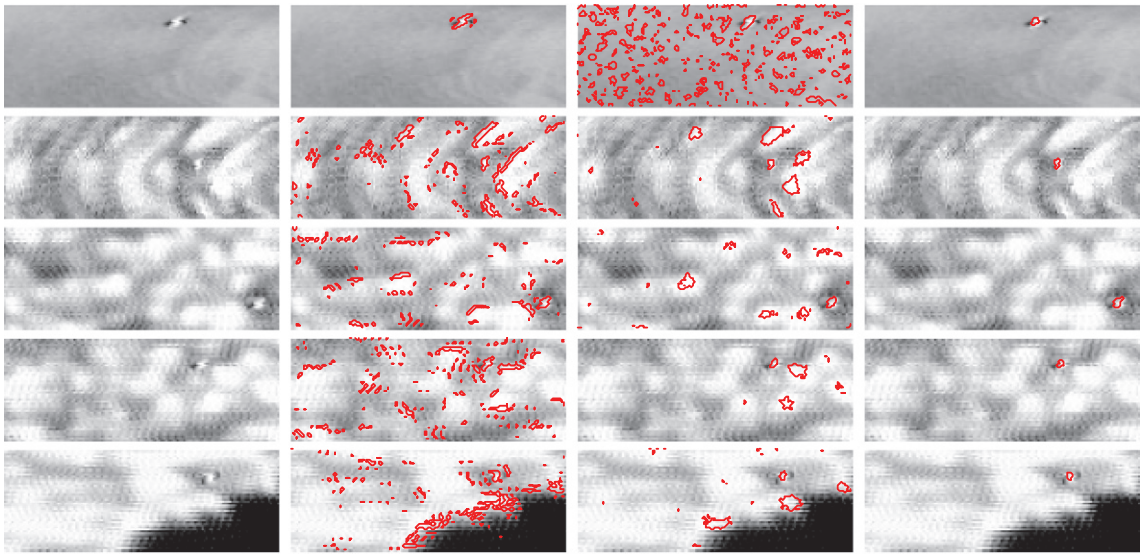

Fig. 3. Detective IR samples under clutter background using the proposed method ($v = 0.0005$). The first column: original infrared images under different clutter background. The second column: Intermediate evolution results at the 1st iteration. The third column: Intermediate evolution results at the 5th iteration. The forth column: Finally evolution results at the 40th iteration.

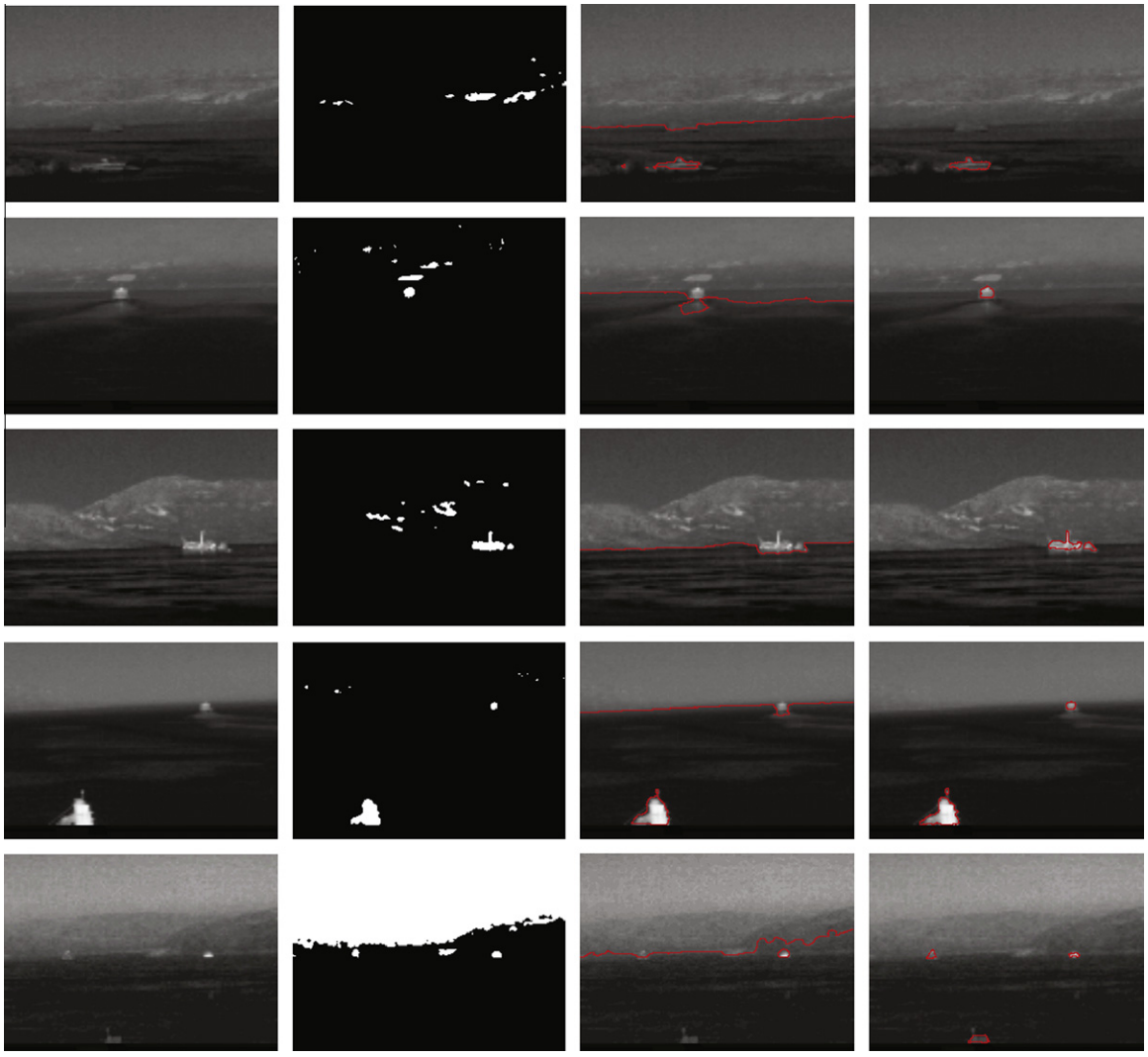

Fig. 4. Detective IR samples under sky–mountain–water background using the 2-D maximum entropy model [3], the improved CV model [11] and the propose model. The first column: Original infrared images under different sky–mountain–water background. The second column: results of the 2-D maximum entropy model. The third column: Finally results at the 10,000th iteration of improved CV model. The forth column: Finally results at the 40th iteration of our model with parameters v = 0.004, 0.004, 0.002, 0.002 and 0.005, respectively (from the top to the bottom).

the results of level set evolution. In addition, the improved CV model cannot extract the weak object contour at the bottom of the last image. Due to the introduction of multi-channel information with structure tensor for our model, it avoids the influence of mountain–water line. We can see from the forth column of Fig. 4, our model extract successfully all the boats contours under sky–mountain–water background.

5. Conclusion

A tensor diffusion level set method is proposed to extract IR targets contour under complex background. This framework utilizes image tensor diffusion operator to integrate the information at each image location, which drives the level set function up or down in transition region, and located targets edges. While a weighted $p(\lambda_1, \lambda_2)$-Dirichlet integral as regularity term is presented to diminish the influence of image 'clutter' and noise. So the targets contours in image with complex background can be efficiently extraction. Another merit of the proposed method is robust to initial conditions. Experimental results on IR images with different backgrounds demonstrate the effectiveness of the tensor diffusion level set method.

Acknowledgment

The authors thank the anonymous reviewers for their valuable comments and suggestions.

References

[1] J. Shaik, K.M. Iftekharuddin, Detection and tracking of targets in infrared images using Bayesian techniques, Optics & Laser Technology 41 (2009) 832–842.
[2] L. Yang, J. Yang, K. Yang, Adaptive detection for infrared small target under sea–sky complex background, Electronics Letters 40 (17) (2004) 1083–1085.
[3] F. Du, W. Shi, L. Chen, Y. Deng, Z. Zhu, Infrared image segmentation with 2-D maximum entropy method based on particle swarm optimization, Pattern Recognition Letters 26 (2005) 597–603.
[4] S.R. Neves, E.A.B. da Silva, G.V. Mendonca, Wavelet–watershed automatic infrared image segmentation method, Electronics Letters 39 (12) (2003) 903–904.
[5] L.Q. Li, Y.Y. Tang, Wavelet–Hough transform and its applications to edge and target detections, International Journal of Wavelets, Multi-Resolution and Information Processing 4 (2006) 567–587.
[6] P.B. Chapple, D.C. Bertilone, R.S. Caprai, G.N. Newsam, Stochastic model-based processing for detection of small targets in non-Gaussian natural imagery, IEEE Transactions on Image Processing 10 (4) (2001) 554–564.
[7] Y. Chen, X. Liu, Q. Huang, Real-time detection of rapid moving infrared target on variation background, Infrared Physics & Technology 51 (2008) 146–151.
[8] T. Chan, L. Vese, Active contours without edges, IEEE Transactions on Image Processing 10 (2) (2001) 266–277.

[9] C. Li, C. Xu, C. Gui, M.D. Fox, Level set formulation without re-initialization: a new variational formulation, in: Proceedings of IEEE Conference on Computer Vision and Pattern Recognition (CVPR), vol. 1, 2005, pp. 430–436.
[10] C. Li, C. Kao, J.C. Gore, Z. Ding, Minimization of region-scalable fitting energy for image segmentation, IEEE Transactions on Image Processing 17 (10) (2008) 1940–1949.
[11] X. Mei, J. Lin, L. Zhang, L. Xia, Infrared image segmentation algorithm based on improved variational level set model, in: Proceedings of IEEE International Conference on Mechatronics and Automation, 2007, pp. 1224–1228.
[12] Y. Huang, J. Wu, Infrared thermal image segmentations employing the multilayer level set method for non-destructive evaluation of layered structures, NDT&E International 43 (2010) 34–44.
[13] L. Wang, C. Li, Q. Sun, D. Xia, C. Kao, Active contours driven by local and global intensity fitting energy with application to brain MR image segmentation, Computerized Medical imaging and Graphics 33 (2009) 520–531.
[14] L. He, Z. Peng, B. Everding, X. Wang, C. Han, K. Weiss, W. Wee, A comparative study of deformable contour methods on medical image segmentation, Image and Vision Computing 26 (2008) 141–163.
[15] S. Osher, J.A. Sethian, Fronts propagating with curvature dependent speed: algorithms based on Hamilton–Jacobi formulations, Journal of Computational Physics 79 (1988) 12–49.
[16] V. Caselles, F. Catte, T. Coll, F. Dibos, A geometric model for active contours in image processing, Numerische Mathematik 66 (1993) 1–31.
[17] R. Malladi, J.A. Sethian, B.C. Vemuri, Shape modeling with front propagation: a level set approach, IEEE Transactions on Pattern Analysis and Machine Intelligence 17 (1995) 158–175.
[18] J. Weickert, Anisotropic Diffusion in Image Processing, Teubner Verlag, Stuttgart, 1998.
[19] T. Brox, J. Weickert, B. Burgeth, P. Mrazek, Nonlinear structure tensor, Image and Vision Computing 24 (1) (2006) 41–55.
[20] M. Rousson, T. Brox, R. Deriche, Active unsupervised texture segmentation on a diffusion based feature space, in: IEEE Computer Society Conference on Computer Vision and Pattern Recognition, 2003, pp. 699–704.
[21] H. Li, Y. Wei, L. Li, Y.Y. Tang, Infrared moving target detection and tracking based on tensor locality preserving projection, Infrared Physics & Technology 53 (2010) 77–83.
[22] G. Chung, L.A. Vese, Image segmentation using a multilayer level-set approach, Computing and Visualization in Science 12 (2009) 267–285.
[23] B. Zhou, C.L. Mu, Level set evolution for boundary extraction based on a p-Laplace equation, Applied Mathematical Modelling 34 (12) (2010) 3910–3916.
[24] J.E. Solem, N.C. Overgaard, A. Heyden, Initialization techniques for segmentation with the Chan–Vese model, in: Proceedings of 18th International Conference on Pattern Recognition (ICPR'06), vol. 2, 2006, pp. 171–174.
[25] R.B. Xia, W.J. Liu, J.B. Zhao, L. Li, An optimal initialization technique for improving the segmentation performance of Chan–Vese model, in: Proceedings of the IEEE International Conference on Automation and Logistics, 2007, pp. 411–415.
[26] M. Li, C. He, Y. Zhan, Adaptive level-set evolution without initial contours for image segmentation, Journal of Electronic Imaging 20 (023004) (2011), doi:10.1117/1.3574770.